Interaction between the Two Conserved Single-Stranded Regions at the Decoding Site of Small Subunit Ribosomal RNA Is Essential for Ribosome Function

Philip R. Cunningham,‡ Kelvin Nurse, Andrey Bakin, Carl J. Weitzmann,§ Michelle Pflumm, and James Ofengand*

Roche Institute of Molecular Biology, Roche Research Center, Nutley, New Jersey 07110

Received July 27, 1992

ABSTRACT: Formation of the tertiary base pair G1401:C1501, which brings together two universally present and highly sequence-conserved single-stranded segments of small subunit ribosomal RNA, is essential for ribosome function. It was previously reported that mutation of G1401 inactivated all in vitro functions of the ribosome [Cunningham et al. (1992) *Biochemistry 31*, 7629–7637]. Here we show that mutation of C1501 to G was equally inactivating but that the double mutant C1401:G1501 with the base pair reversed had virtually full activity for tRNA binding to the P, A, and I sites and for peptide bond formation. Initiation-dependent formation of the first peptide bond remained 70–85% inhibited, despite full 70S initiation complex formation ability as evidenced by the ability to form fMet-puromycin. These results suggest that the defect in formation of the first peptide bond lies in filling the initial A site, A_i, rather than the subsequent elongation A sites, A_e. An increased mobility around the anticodon was detected by UV cross-linking of the anticodon of P-site-bound tRNA to C1399 as well as to the expected C1400. These findings provide the first experimental evidence for the existence of the G1401:C1501 base pair and show that this base pair, located at the decoding site, is essential for function. The structural implications of tertiary base pair formation are discussed.

It is now well established that ribosomal RNA plays an important functional role in ribosomal protein synthesis (Noller, 1991). The first clear evidence for the involvement of 16S RNA in the decoding function other than at the Shine–Dalgarno site was the demonstration that the C1400 residue could be cross-linked to the 5′-anticodon base of P-site-bound tRNA (Schwartz & Ofengand, 1978; Ofengand et al., 1986). This result placed a specific rRNA base in close proximity to the site of codon–anticodon interaction. Subsequent cross-linking studies confirmed the presence of the 1391–1408 region of 16S RNA near to mRNA bases 4–11 residues from the first base of the codon being read (Tate et al., 1990; Rinke-Appel et al., 1991). The functional involvement of 16S RNA implied by this close proximity to mRNA *at the decoding site* was confirmed by the striking effect of rRNA mutations made in the vicinity of the cross-linked bases both in vitro (Denman et al., 1989a; Cunningham et al., 1990a) and in vivo (Rottmann et al., 1988; Hui et al., 1988; Thomas et al., 1988). The other primary function of the ribosome, namely, catalysis of peptide bond function, has recently been shown to also be an rRNA-directed event, in this case involving 23S RNA (Noller et al., 1992).

We have previously reported the detection of a "keystone" nucleotide in 16S RNA, G1401, which is located at the decoding site adjacent to the cross-linkable C1400 residue. Substitution at this site by any other base caused the virtually complete loss of all tRNA binding and protein synthesis function (Cunningham et al., 1992). This result was all the more remarkable since mutation of either adjacent base, C1400 or C1402, had little or no effect. In order to explain this strong but highly specific inhibition, we postulated that the tertiary interaction between G1401 and C1501 (Figure 1), proposed by Gutell and co-workers on the basis of comparative sequence analysis (Gutell et al., 1985; Gutell & Woese, 1990), was essential for the proper functioning of the ribosome.

A prediction from this model would be that (a) breaking the base pair by mutating C1501 would be as deleterious as mutating G1401 and (b) re-forming the base pair by construction of the double mutant C1401:G1501 might restore function. In this work we show that both predictions are correct and discuss how these conclusions bear on the three-dimensional structure of the decoding site of a functioning ribosome. Preliminary accounts of this work have appeared (Cunningham et al., 1991a,b).

EXPERIMENTAL PROCEDURES

Materials

All materials not otherwise mentioned were obtained or prepared as described in Denman et al. (1989a,b) or Cunningham et al. (1990b). pWK1, a derivative of pUC19 capable of directing the in vitro synthesis of full-length 16S RNA by T7 RNA polymerase, has been described elsewhere (Kryzosiak et al., 1988). The mixture of 30S ribosomal proteins (TP30) was prepared as described previously (Kryzosiak et al., 1987) except that exposure to acetic acid was reduced from 45 to 15 min. mRNA and the high salt wash (HSW) containing crude initiation factors for the I-site and fMet-Val assays were prepared according to Cunningham et al. (1990b). mRNA-S was prepared in the same way as for the standard mRNA except that the plasmid template was linearized with *Hin*dIII, resulting in an mRNA product 58 nucleotides long. This RNA has 23 coding nucleotides compared to 732 for the standard mRNA preparation. RD buffer is 20 mM Hepes, pH 7.5, 100 mM NH_4Cl, 20 mM $Mg(OAc)_2$, and 5 mM mercaptoethanol. $tRNA^{Leu5}$ was obtained from Subriden RNA.

In Vitro Synthesis of Mutant Ribosomes

16S rDNA mutants C1401 and G1501 and the double mutant C1401:G1501 were constructed following procedures

* To whom correspondence should be addressed.
‡ Present address: Department of Biological Sciences, Wayne State University, Detroit, MI 48202.
§ Present address: Pall Corp., Glen Cove, NY 11542.

0006-2960/92/0431-12012$03.00/0 © 1992 American Chemical Society

described previously (Cunningham et al., 1990b, 1992) and verified by sequence analysis. Transcription of the gene by T7 RNA polymerase was as described (Cunningham et al., 1991c) except that 5 mM NTP, 3000 units/mL T7 RNA polymerase, and 7.1 nM (20 μg/mL) linearized plasmid were used. The synthesized RNA was isolated by the phenol-S200 method (Cunningham et al., 1991d) and characterized by glyoxal–DMSO denaturing gel electrophoresis (Denman et al., 1989b). Ribosome reconstitution on a preparative scale was performed according to Cunningham et al. (1990b). The RNA of each mutant ribosome was reextractedand sequenced (Bakin & Ofengand, 1992) to verify its mutant nature.

Functional Assays

70S Formation. Reaction mixtures containing 100 nM 50S subunits and 67 nM 30S subunits in 50 mM Hepes, pH 7.5, 50 mM NH_4Cl, 15 mM $Mg(OAc)_2$, 5 mM DTT, and 25 μg/mL poly(U) were preincubated at 37 °C for 10 min, followed by addition of 100 nM deacylated $tRNA^{Phe}$ and incubation for 20 min. The samples, 0.2 mL, were layered on sucrose gradients containing 20 mM Hepes, pH 7.5, 100 mM NH_4Cl, and 15 mM $Mg(OAc)_2$ and analyzed as described by Denman et al. (1989b).

P-Site Binding of tRNA. Reaction mixtures contained 50 mM Hepes, pH 7.5, 100 mM NH_4Cl, 15 mM $Mg(OAc)_2$, 5 mM DTT, 20 μg/mL poly(U_3,G), 100 nM 50S subunits, and 67 nM 30S subunits in 50 μL. After 10-min incubation at 37 °C, 115 nM Ac[^{3}H]Val-tRNA was added and incubation continued for 20 min longer. Duplicate samples were analyzed as described (Kryzosiak et al., 1987). Values for the complete system minus 30S subunits were used as blanks. Blanks with poly(U_3,G) omitted were approximately the same as those lacking 30S subunits.

A-Site Binding of tRNA. This was performed in three steps. In step 1, the P site was filled with uncharged $tRNA^{Phe}$ by incubating 100 nM activated 30S (Zamir et al., 1974) plus 160 nM 50S with 2000 nM uncharged $tRNA^{Phe}$ in a 40-μL reaction mixture containing TC buffer (50 mM Hepes, pH 7.5, 75 mM NH_4Cl, 75 mM KCl), 14 mM $Mg(OAc)_2$, 2.5 mM mercaptoethanol, and 50 μg/mL poly(U) for 10 min at 37 °C. In step 2, the ternary complex was prepared by incubating 2 mM GTP with or without 4.5 μM EFTu in TC buffer containing 5 mM $Mg(OAc)_2$ for 15 min at 37 °C. [^{3}H]Phe-tRNA, 1000 nM, was added and incubation continued for 5 min more. In step 3, 40 μL of the step 1 mixture was combined with 10 μL of the step 2 mixture and incubated for 20 min at 37 °C. The final concentrations were 12 mM $Mg(OAc)_2$, 0.4 mM GTP, 40 μg/mL poly(U), 900 nM EFTu, 1600 nM $tRNA^{Phe}$, 200 nM [^{3}H]Phe-tRNA, and 80 nM 30S in TC buffer. Analysis was performed in duplicate as previously described (Denman et al., 1989a). Binding in the absence of EFTu was <10% of that in its presence. Blank reactions lacked 30S subunits.

Polyphenylalanine Synthesis. The reaction was performed in two stages. In the first stage, 50 nM activated 30S, 80 nM activated 50S, and 250 μg/mL poly(U) were incubated in 12 mM Hepes, pH 7.5, 58 mM NH_4Cl, 15 mM $Mg(OAc)_2$, and 3 mM mercaptoethanol for 5 min at 37 °C. The reaction mixture was adjusted to contain 45 mM Bicine plus 5 mM Hepes, pH 7.5, 50 mM NH_4Cl, 15 mM $Mg(OAc)_2$, 5 mM phosphoenolpyruvate, 2 mM ATP, 5 mM DTT, 80 μg/mL pyruvate kinase (Boehringer), 1 mM GTP, 600 nM EFTu, 30 μg/mL EFG, 1000 nM [^{3}H]Phe-tRNA, 20 nM activated 30S subunits, 33 nM 50S, and 100 μg/mL poly(U) and incubation continued at 37 °C. Samples (10–35 μL) were withdrawn at the indicated times, 1.5 mL of 10% TCA containing 2% casamino acids (Difco) was added, and the mixture was heated at 90 °C for 15 min. After cooling, the samples were passed through nitrocellulose filters, washed with 5% TCA containing 2% casamino acids, and counted after the filters were dissolved. Values were corrected for the small amount of reaction found in the absence of 30S subunits.

30S Initiation Complex Formation (I Site). Reaction mixtures in duplicate contained 50 mM Hepes, pH 7.5, 135 mM NH_4Cl, 16 mM $Mg(OAc)_2$, 5 mM DTT, 1.4 mM GTP, 300 units/mL RNasin (Promega), 250 nM mRNA, 1.3 mg/mL HSW, 250 nM f[^{35}S]Met- or f[^{3}H]Met-tRNA, and 136 nM 30S subunits in a volume of 25 μL. After 20 min at 37 °C, the mixtures were filtered as for P-site binding. Values from reactions lacking 30S subunits were subtracted. Binding in the absence of HSW was <10% of that in its presence.

fMet–Puromycin Formation. Reaction mixtures were as above except for 12 mM $Mg(OAc)_2$, 600 units/mL RNasin, 700 nM RNA-S, 200 nM fMet-tRNA, 0.33 mg/mL HSW, and 120 nM 30S subunits. After incubation for 5 min at 37 °C, 50S subunits were added to a molar ratio of 50S/30S of 1.5. After a second 5-min incubation at 37 °C, the reaction mixture was chilled to 0 °C, puromycin was added to 1 mM, and incubation was continued at 0 °C. Aliquots (30 μL) were removed as a function of time, 40 μL of 2 M NaOAc, pH 5.6, and 330 μL of H_2O were added, and the mixture was extracted with 850 μL of ethyl acetate. After vortexing for 1 min, 550 μL of the ethyl acetate layer was removed for counting. Noncovalently bound fMet-tRNA was measured after the first and second 37 °C incubation by filtration as for P-site binding. Within experimental error, the two sets of binding values were the same. Values from reactions lacking 30S subunits were subtracted as the blank. fMet-tRNA binding values obtained in this assay were the same as in the standard assay.

fMet-Val Dipeptide Synthesis. The reaction mixture in 35 μL contained 50 mM Hepes, pH 7.5, 34 mM NH_4OAc, 21 mM NH_4Cl, 39 mM KOAc, 6 mM KCl, 7.5 mM $Mg(OAc)_2$, 1.2 mM spermidine, 5 mM DTT, 27 mM potassium phosphoenolpyruvate, 11 μg/mL pyruvate kinase, 3 mM ATP, 0.3 mM GTP, 250 units/mL RNasin, 4.3% poly(ethylene glycol) 8000, 0.16 mg/mL HSW, 700 nM EFTu, 500 nM mRNA, 600 nM unlabeled fMet-tRNA, 300 nM [^{3}H]Val-tRNA, 10–50 nM 30S subunits, and a 1.5-fold excess of 50S subunits over 30S. After incubation for 90 min at 37 °C, the reaction was stopped by addition of 13 μL of 0.5 M KOH. After 15 min at 50 °C, 0.5 mL of 0.05 M HCl was added; the sample was applied to a 0.6 × 4 cm column of Dowex-50-H^+ equilibrated in water, eluted with 3 × 0.5 mL of water, and counted. Values were corrected for an 82% elution efficiency for fMet-Val. Blank reactions without 30S subunits were subtracted. fMet-Val formation was dependent on the presence of HSW, 30S, 50S, fMet-tRNA, and mRNA. For the kinetic experiment of Figure 4, the reaction mixture minus 30S and 50S was preincubated for 30 min at 37 °C. The reaction was started by addition of the 30S and 50S subunits preincubated for 30 min at 37 °C in RD buffer.

Misincorporation. This assay was performed as for polyphenylalanine synthesis with the following modifications. In the first stage, streptomycin was included at 6 μg/mL where indicated. In the second stage, 1200 nM [^{3}H]Leu-$tRNA^{Leu5}$ (anticodon N*AA) was added, and the [^{3}H]Phe-tRNA was replaced by 800 nM [^{14}C]Phe-tRNA. Samples (25–35 μL) were taken at 5, 10, and 15 min. The reaction was stopped

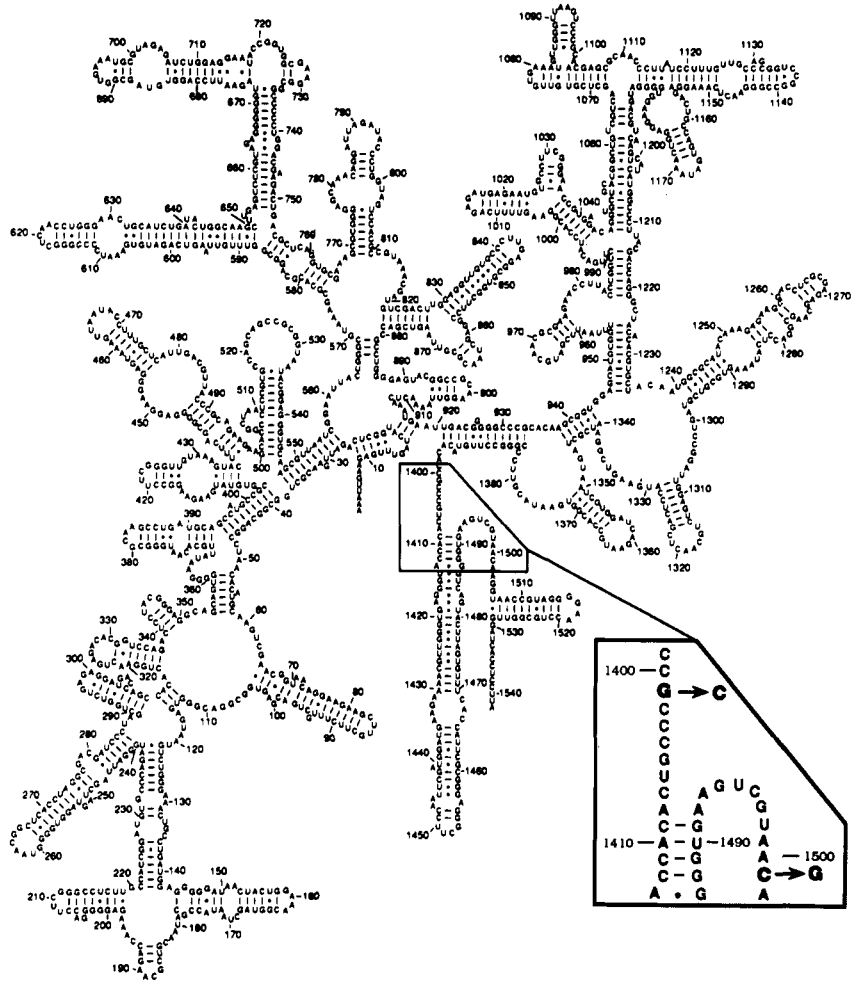

FIGURE 1: Location of the mutated nucleotides. The secondary structure of *E. coli* 16S RNA is according to Stern et al. (1989). The inset shows the sites of the mutations described in this work in boldface type. The two positions, 1401 and 1501, are involved in a long-range interaction.

by addition of 100 μL of water followed by 1.5 mL of 10% TCA containing 2% casamino acids (Difco). After being heated to 90 °C for 15 min, the samples were collected on nitrocellulose filters and washed three times with 5 mL of the same TCA solution.

Cross-Linking

After P-site binding of the AcVal-tRNA as described above, the samples were irradiated for 30 min at 0 °C with the full set of 16 300-nm lamps in the Rayonet photoreactor using 1 cm of Pyrex glass as a low-wavelength cutoff filter. This time is sufficient for maximum cross-linking (Denman et al., 1988). After removal of an aliquot for measurement of noncovalent binding (Kryzosiak et al., 1987), the sample was precipitated with 2% KOAc, pH 5, and 67% EtOH, and the pellet was dissolved in 20 mM Hepes, pH 7.5, 100 mM LiCl, 2 mM EDTA, and 1% SDS by incubation at 37 °C for 5 min. The samples was applied to a 1 × 26 cm column of Sephacryl S-200 at 23 °C in the same buffer except 0.1% SDS and eluted at 0.2 mL/min. Fractions of 0.25 mL were taken for counting. The early-eluting peak of tRNA cross-linked to rRNA (Figure 6A) was quantitated after correction for the irradiation-independent blank. Percent cross-linking is the amount of AcVal-tRNA found in this peak divided by the amount noncovalently bound to ribosomes as measured by the standard P-site binding assay.

Reverse Transcription Analysis of the Site of Cross-Linking

The tRNA–rRNA covalent complex in the 1% SDS buffer described above was extracted with an equal volume of $CHCl_3$-equilibrated phenol, the phenol layer was washed, the combined aqueous phases were extracted twice with $CHCl_3$, and the RNA was precipitated with 2% KOAc, pH 5, and 67% EtOH. The pellet was dissolved in 2% KOAc, pH 5, reprecipitated with 67% EtOH, and washed with 70% EtOH. Primer extension was carried out essentially as described by Bakin and Ofengand (1992), using a primer complementary to residues 1526–1542. After the labeling step, 1 μL of 0.4, 2, or 4 mM dNTP chase solution was added, and the incubation was continued at 37 °C for 45 min. The reaction was stopped, and samples were analyzed as previously described (Bakin & Ofengand, 1992).

RESULTS

Location of the Tertiary Base Pair G1401:C1501. The two positions mutated in this work are shown in Figure 1. Although they occur 100 nucleotides apart in the pairing sequence, it was postulated, on the basis of the rather weak phylogenetic evidence summarized in Table I, that they might form a standard base pair (b in Figure 8) in the ribosome (Gutell et al., 1985; Gutell & Woese, 1990). Because these positions are so highly conserved, only 6 true A1401:U1501 base-pair replacements are found out of some 630 sequences, and

Table I: Sequence Covariance between Positions 1401 and 1501 in Small Subunit rRNAs

1400						1500						
C	A	C	C	G	C	C	C	G	U	C	•••	A A G U C G U A A C A A G G

Archetype sequence[a] ~600 species

Variant Mitochondria[b]

A			A		U								A		U		U							*A. nidulans*
A		U	A		U	A						U	A		U		C	A					*S. cerevisiae*
A			U	A		U							A		U									*S. pombe*
A			A		U								A		U		C							*P. anserina*
A		U	A	U		A					U			G	U		A							*C. elegans*
A		U	A	U		A					U			G	U		A							*A. suum*
U	G	U	U			A	C			C	G	U	C	G	U		U	U						*T. brucei*
U	G	U	U			A	C			C	G	U	C	G	U		U	U						*C. fasciculata*
U	G	U	U			A	C			C	G	U	C	G	U		U	U						*L. tarentolae*
U	G	U	U			A	C			C	G	U	C	G	U		U	U						*Leptomonas sp.*

[a] All eukaryotes, archaebacteria, eubacteria, chloroplasts, and 16 species of mitochondria. [b] Mitochondrial ribosomes variant at 1401 and/or 1501. Nineteen other species are variant between 1397–1407 and 1492–1505 but not at either 1401 or 1501.

these six are all in mitochondrial ribosomes. The four G1401:U1501 pairs are all in trypanosome species, and in any case since only a single mutational event is required, their occurrence is not as significant.

The base-pairing proposal was intriguing for both structural and functional reasons. Structurally, current information about the topographical dispositions of the two single-stranded regions in which G1401 and C1501 reside places them on either side of the cleft of the 30S subunit (see Figure 8). A base-pairing interaction of the Watson–Crick type would therefore require that either the cleft close up so that the two sequences would be juxtaposed at least transiently or that one or both RNA strands loop out, possibly also transiently, in order to cross the cleft. Functionally, the tertiary base pair proposal would provide a rationale for the previously reported findings that replacement of G1401 by any other nucleotide inactivated all ribosome function, whereas substitutions on either side, namely, at C1400 or C1402, had little or no effect (Cunningham et al., 1992). In view of the potential for obtaining both structural and functional information of relevance to the mechanism decoding, the existence of the G1401:C1501 base pair was tested by mutational analysis.

Preparation and Characterization of the Mutant Ribosomes. The "synthetic" ribosome system (Kryzosiak et al., 1987) was used to explore the in vitro functional behavior of C1401, G1501, and the reciprocal base-pair double mutant C1401:G1501. This system has proven its utility in other mutational investigations (Denman et al., 1989a; Cunningham et al., 1990a,b, 1992). In this system, mutations which are introduced into the 16S RNA gene by cassette mutagenesis are transferred into 16S RNA by in vitro transcription using T7 RNA polymerase. The RNA is then reconstituted in vitro with isolated 30S proteins to yield a fully mutant particle. The advantages of this largely in vitro system have been detailed elsewhere (Cunningham et al., 1992).

The ability of the mutants G1501 and C1401:G1501 to be reconstituted in this fashion is shown in Figure 2. Clearly, both mutants were reconstituted as well as the wild-type RNA, here denoted G1401:C1501 or Syn. However, all three synthetic particles, represented by the A_{260} peaks, were more heterogeneous than the ^{32}P marker of control isolated 30S. This has been ascribed to the absence of base modification, methylation, and/or pseudouridylation, in the synthetic RNA (Cunningham et al., 1991d). The reconstitution behavior of

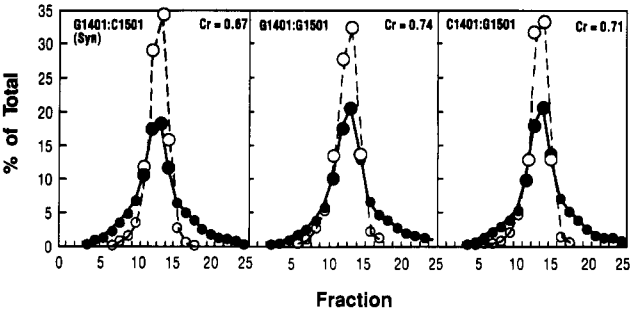

FIGURE 2: In vitro reconstitution of wild-type and mutant ribosomes. Isolation and analysis were be velocity centrifugation through a sucrose gradient. The direction of sedimentation is from right to left. Symbols: filled circles, A_{260}; open circles, marker [^{32}P]30S ribosomes. Normalization of the curves and calculation of the coefficient of reconstitution, C_r, were as described previously (Cunningham et al., 1990b, 1992). The fractions pooled for subsequent functional tests are shown by the larger symbols.

Table II: Protein Content of Mutant Reconstituted 30S Subunits[a]

protein	C1401[b]	G1501	C1401:G1501
S2	1.1	0.5	0.6
S3	0.9	1.1	1.2
S4	1.0	0.9	0.9
S5	1.0	1.1	1.1
S6	1.2	1.2	1.2
S7	0.9	0.9	1.0
S8	1.0	0.9	1.0
S9	1.0	1.1	1.1
S10	1.2	1.0	1.2
S11	1.1	1.1	0.9
S12	1.1	1.1	1.0
S13	1.0	1.2	1.1
S14	0.9	0.9	1.1
S15	1.0	1.0	1.0
S16	1.0	0.9	0.9
S17	1.1	0.9	0.8
S18	1.1	1.0	1.0
S19	1.0	0.9	1.0
S20	1.0	1.0	0.9
S21	0.9	0.8	0.8

[a] Values for the three mutants are expressed as protein/RNA molar ratios, normalized for each protein to reconstituted nonmutant synthetic 30S (Cunningham et al., 1990b). Values <0.8 or >1.2 are underlined. [b] These values were reported previously (Cunningham et al., 1992).

C1401, which was equivalent to those of Figure 2, was reported previously (Cunningham et al., 1992). Thus the very different functional behavior of these mutants (see below) cannot be explained by major differences in the ability to reconstitute.

When considering the effect of RNA mutations on ribosome function, it is important to quantitate the amount of ribosomal proteins present in the mutant particle. Clearly, the mutant particles must at a minimum retain all their proteins if functional effects are to be ascribed to a single base change in the RNA. Table II shows that this is the case for the mutants studied here. The only deviation from unit stoichiometry was found with S2, but since both G1501 and C1401:G1501 were low yet have very different functional behavior (see below), there does not appear to be any functional correlation with the decrease in S2. Moreover, C1401, which has a full amount of S2, was as inactive as G1501.

Functional Behavior of Mutant Ribosomes. Six different assays of ribosomal function in protein synthesis, described in detail previously (Denman et al., 1989a; Cunningham et al., 1990b, 1992), were used (Table III). Note that the fMet-Val assay measured the ability to initiate and form the first peptide bond while the poly(Phe) assay measured peptide bond formation in the absence of initiation. The I-site (30S initiation

Table III: Functional Effects of Site-Specific Nucleotide Substitutions at Positions 1401 and 1501[a]

	mutation position				tRNA binding			peptide synthesis	
	1401		1501	subunit association	P site	A site	I site	poly(Phe)	fMet-Val
(1) normal	G	≡	C	100	100	100	100	100	100
(2) mutant	C		C	40	5	20	5	5	<5
					20	20	5	15	10
(3) mutant	G		G	65	15	25	20	20	<5
					20	15	5	5	5
(4) double mutant	C	≡	G	90	40	85	55	110	5
					90	95	85	130	30
					70	100	75	115	15
calculated	(2)	×	(3)	25	≤5	≤5	<5	<5	<5

[a] Values are expressed as percent of wild-type synthetic 30S subunit activity to the nearest 5%. 100% corresponds to 77% for subunit association, 0.17, 0.26, and 0.20 pmol of tRNA bound/pmol of 30S for P-, A-, and I-site binding, respectively, 3.37 pmol of Phe/pmol of 30S per 10 min for poly(Phe) synthesis, and 2.87 pmol of fMet-Val/pmol of 30S for fMet-Val synthesis. The different rows of numbers for each mutant represent values obtained for independent reconstitutions. The calculated value was obtained as the % value for C1401 × the %/100 value for G1501.

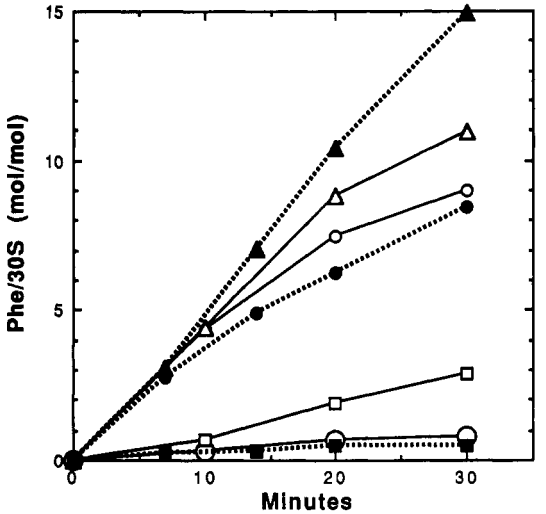

FIGURE 3: Polyphenylalanine synthesis by the mutant ribosomes. The assay was carried out as described under Experimental Procedures for the indicated times. Symbols: solid line, open symbols, reconstitution I; dashed line, filled symbols, reconstitution II; (○, ●) Syn; (◯) C1401; (□, ■) G1501; (△, ▲) C1401:G1501.

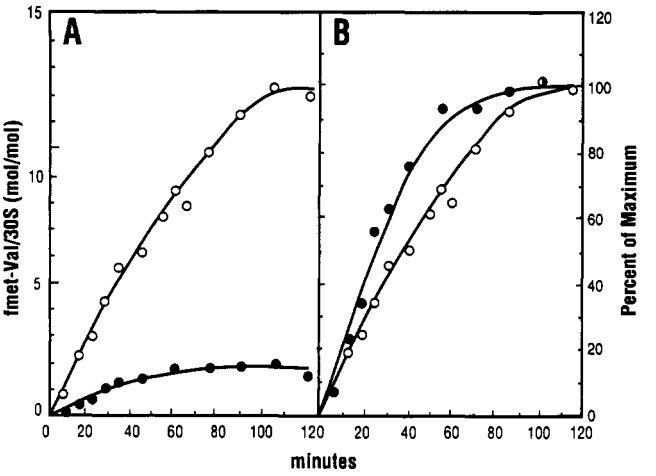

FIGURE 4: Kinetics of fMet-Val synthesis. (Panel A) Rate of synthesis of fMet-Val with nonmutant Syn (○) or double mutant C1401:G1501 (●). (Panel B) Data of panel A expressed as percent of each plateau value.

complex formation) assay was the only one which was not dependent on added 50S subunits. Being independent of prior formation of a 70S couple, it allows monitoring of mutational effects on function separate from subunit association. Each assay was adjusted to make the amount of product proportional to the amount of 30S subunit added. Therefore, the values given in Table III are the average values of an undoubtedly functionally heterogeneous population of 30S particles rather than being those of the most active subpopulation, which is what is measured in ribosome excess.

The first functional test applied was that classic of protein synthesis, poly(U)-dependent synthesis of polyphenylalanine (Figure 3). Two independent reconstitution sets are shown. The wild-type reconstituted control (Syn) makes polyphenylalanine linearly for 20–30 min. As expected from previous work (Cunningham et al., 1992), C1401 was inactive. Fulfilling both predictions made in the introduction, G1501 was also inactive, while the reciprocal double mutant C1401:G1501 was fully active. This result satisfies the classic condition for demonstrating a base pair, namely, that the appropriate double mutant can be substituted. The interaction appears to be of the Watson–Crick type, since the pairs C1401:C1501, A1401:C1501, U1401:C1501, and G1401:G1501 were all inactive (Cunningham et al., 1992). Other combinations such as A:U, U:A, G:U, U:G, and C:A remain to be tested.

We next investigated other partial reactions of the ribosomal protein synthesis cycle. We previously showed that mutation of G1401 to C1401 caused the loss of all measured functions (Cunningham et al., 1992), and this was confirmed in Table III. The second row shows the average of values obtained previously (it differs slightly from the values in that report because of additional data), while the first row shows a reconstitution made at the same time as the first row of G1501 and of C1401:G1501. Clearly C1401 is reproducibly inactive.

G1501 was also inactive in all the tested functions. This represents only the second site known to us (the other is 1401) where a single base change causes the virtually complete loss of all tRNA binding and protein synthesis functions. The double mutant C1401:G1501 was, predictably, reactivated for all functions, although as the table shows, there was some variation from function to function and from reconstitution to reconstitution (three independent ones are shown in Table III). Nevertheless, as the calculated value for independent events shows, even the poorest activity was considerably higher than that predicted if the two mutational sites were unlinked. The only exception to this behavior is fMet-Val formation. This activity did not return to any appreciable extent in the double mutant. In order to show this more clearly, the kinetics of fMet-Val formation were determined (Figure 4). Panel A shows the rate of synthesis of fMet-Val by the control and C1401:G1501 mutant. Clearly the double mutant has only low activity although the kinetic course is like that of the control. This is more clearly seen in panel B, where the data of panel A are normalized to each plateau value. The very

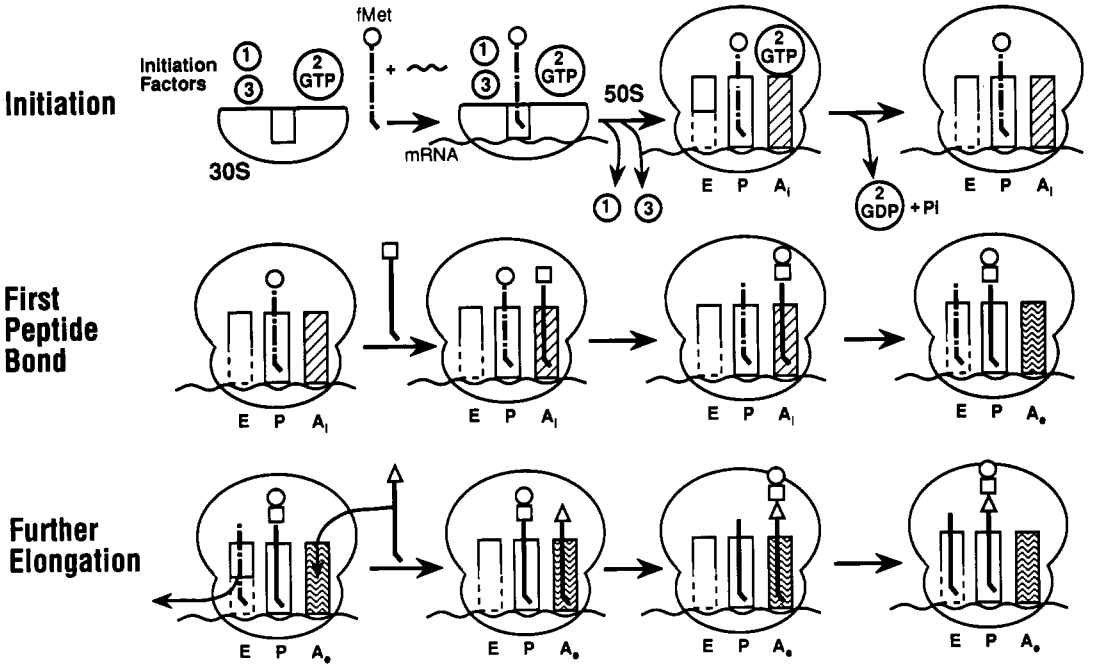

FIGURE 5: State of tRNA binding sites during initiation and elongation on the ribosome. The scheme incorporates current knowledge of ribosomal protein synthesis except for the hybrid site concept of Moazed and Noller (1989). The A site is considered to exist in two states, A_i and A_e, as proposed by Nierhaus and co-workers (Hausner et al., 1988; Nierhaus, 1990).

Table IV: Puromycin Reactivity of 30S–fMet-tRNA Complexes[a]

	fMet-PM/fMet-tRNA bound		
time (min)	isolated G1401:C1501	synthetic G1401:C1501	synthetic C1401:G1501
5	0.79	0.90	1.19
10	0.84	0.93	1.20
15	0.77	0.89	1.14

[a] 30S–fMet-tRNA initiation complexes formed with isolated and synthetic wild-type and double mutant 30S were, after addition of a 1.5-fold excess of 50S subunits and incubation for 5 min at 37 °C, reacted with 1 mM puromycin (PM) at 0 °C for the indicated times. The amount of fMet-tRNA bound to the 30S and 70S complexes was determined by filter binding at 20 mM Mg^{2+} and corrected for the blank value obtained in the absence of 30S subunits. 30S-dependent fMet-PM formation was determined by ethyl acetate extraction. There was no fMet-PM found in the absence of 50S subunits and <7% in the absence of puromycin. The ratio of the amount of fMet-PM formed to the amount of fMet-tRNA bound to the 30S subunit is reported.

similar time courses indicate that the same events are likely to be operative in both cases, but with a much lower percentage of active particles in the case of the double mutant. Specifically, the mutant activity does not appear to be due to an initial reaction at the same rate as the control but which stops prematurely.

Localization of the Defect in fMet-Val Synthesis in the C1401:G1501 Double Mutant. Since fMet-Val synthesis was inhibited while formation of the fMet-tRNA–mRNA–30S initiation complex was not, we were forced to consider later steps of initiation as the site of inhibition. As Figure 5 demonstrates, the block could occur at any number of steps. Several could be eliminated at once if the 30S initiation complex formed with the mutant could be shown to undergo the puromycin reaction since that should mean that the ability to complex with the 50S subunit, to release IFs 1 and 3, to hydrolyze GTP and release IF2, and to form an amide bond is intact (Hershey, 1987). This was the case (Table IV). Remarkably, even at 0 °C, the puromycin reaction was complete in less than 5 min and resulted in the reaction of viturally all of the bound fMet-tRNA. This was also true for isolated natural 30S subunits. Thus the rapidity of the reaction was not due to either the act of reconstitution or the absence of modified bases in the synthetic ribosomes.

Ability of the Double Mutant to Cross-Link to C1400. Formation of the cyclobutane dimer cross-link between cmo^5-U34, 5′-anticodon base of $tRNA^{Val1}$, and C1400 of 16S RNA is sensitive to the stereochemistry of the immediate environment, since it requires the two bases to be parallel to each other and sufficiently close so that the π-orbitals of their respective C_5–C_6 double bonds can interact. This sensitivity was experimentally shown by (a) variation in the yield of cross-link when different tRNA anticodon sequences surrounding the cmo^5U residue were compared (Ofengand et al., 1979; Ofengand & Liou, 1981), (b) the dependence of cross-linking on the *lack* of base pairing of the cmo^5U residue with an mRNA codon (Ofengand & Liou, 1981), (c) variation in the yield of cross-linking when ribosomes from different species were compared (Ofengand et al., 1982; Nurse et al., 1987), and (d) the failure to obtain any cross-linking to the adjacent C residue, C1399 (Ehresmann & Ofengand, 1984). On the other hand, cross-linking yield was not affected by the simultaneous occupancy of the A site (Ofengand et al., 1986) or by omission of the 50S subunit (Denman et al., 1988).

Normally, C1400 is cross-linked when G1401 is present. The position of the cross-link seems to depend more on being 5′ to G1401 than on being at 1400 since insertion of a C or U residue between C1400 and G1401 led to cross-linking with normal kinetics to the inserted base but not to C1400 (Denman et al., 1989b). In the double mutant, there are six C residues from positions 1399–1404. The question was whether in the absence of G1401 any cross-linking would occur and, if it did, to which C residue(s).

Figure 6 shows the results of an experiment in which the yield of cross-linking to the double mutant was compared to that of the wild-type control. The analysis was by gel filtration after disruption of the ribosome by SDS treatment. tRNA after cross-linking to 16S RNA was expected to migrate much faster than non-cross-linked material (Ofengand et al., 1979). As shown in panel A, the appearance of a faster moving peak

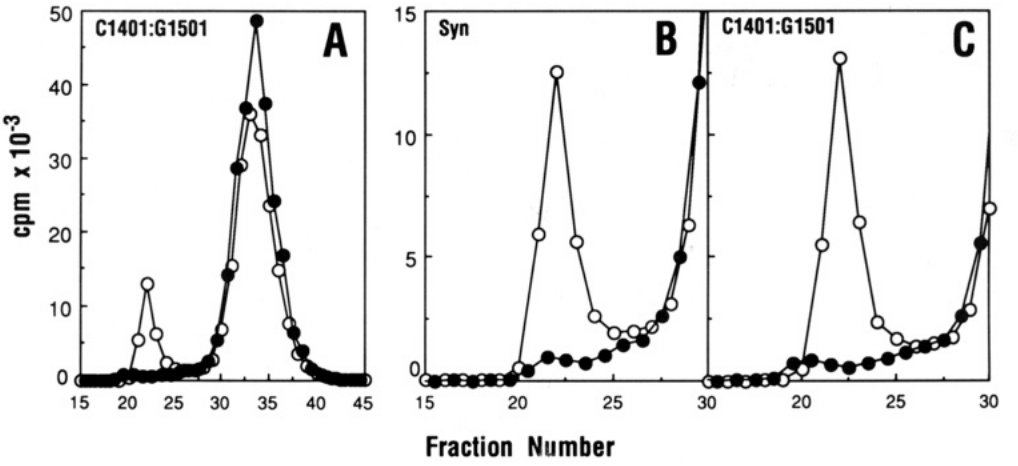

FIGURE 6: Cross-linking of AcVal-tRNA to the P site of normal and double mutant 30S ribosomes. (Panel A) Sephacryl S-200 column chromatography of cross-linked Ac[^{3}H]Val-tRNA–rRNA covalent complexes derived from the mutant C1401:G1501 30S ribosomes. Preparation and analysis were as described under Experimental Procedures. (Panels B and C) Expanded view of the chromatograms for wild-type (Syn) and mutant (C1401:G1501) 30S ribosomes, respectively. Symbols: open circles, plus irradiation; filled circles, minus irradiation.

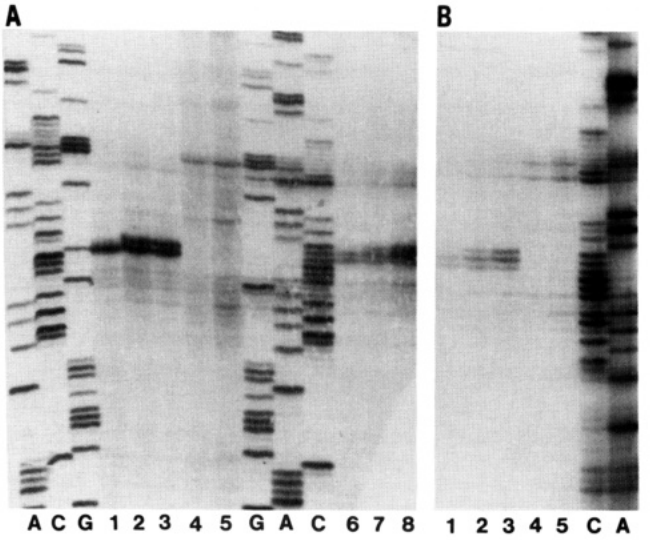

FIGURE 7: Reverse transcription arrest analysis of the cross-link site. (Panel A) lanes A, C, G, 1–5, synthetic control; lanes G, A, C, 6–8, C1401:G1501; lanes 1–3 and 6–8, 50, 250, and 500 μM dNTP in the extensions reaction, respectively; lane 4, 500 μM dNTP minus irradiation; lane 5, 500 μM dNTP minus AcVal-tRNA; lanes A, C, G, and G, A, C, sequencing lanes. (Panel B) Lanes 1–5, C, A, C1401:G1501; lanes 1–3, 50, 250, and 500 μM dNTP in the extension reaction, respectively; lane 4, 250 μM dNTP minus irradiation; lane 5, 250 μM dNTP minus AcVal-tRNA; lanes C, A, sequencing lanes.

of radioactively labeled tRNA was totally dependent on prior irradiation. In panels B and C, this area of the chromatogram is expanded to show both the equivalence of the peak size in control (Syn) and C1401:G1501 ribosomes and the dependence on irradiation. Quantitation of the amount cross-linked yielded 0.099 and 0.097 mol of tRNA/mol of 30S for Syn and C1401:G1501, respectively. From the amount noncovalently bound, 0.167 and 0.148 mol/mol of 30S, respectively, a cross-linking yield of 60% was obtained for the control particles and 66% for the double mutant. The kinetics of cross-linking were not examined in this experiment, but from the irradiation time used, 30 min, and the published kinetics of cross-linking to 30S + 50S in the same apparatus (Denman et al., 1988), the rate could not differ by more than 2-fold.

The site of cross-linking was determined by the transcription arrest procedure (Nurse et al., 1987; Denman et al., 1988, 1989b). As shown in Figure 7, two bands, corresponding to stops at C1400 and G1401, were found in the control, and three stops, at C1399, C1400, and C1401, were detected in the double mutant. All stops were absent when tRNA or irradiation was omitted. The double stop at a single cross-link site in the control is due to the phenomenon of "stuttering" (Nurse et al., 1987; Denman et al., 1988; Ericson & Wollenzien, 1988). The three stops in the double mutant must therefore correspond to a cross-link to C1399 rather than to C1400 in a fraction of the molecules. In agreement with this interpretation, when the dNTP concentration in the reverse transcription reaction was reduced 10-fold, only one strong stop, at G1401, was found in the control while stops at G1401 and C1400 were detected in the double mutant. A similar effect was obtained when the amount of reverse transcriptase was decreased rather than the NTP (data not shown). As the multiple bands are of similar intensity, it appears that the double mutant has sufficient freedom of movement around the decoding site to allow juxtaposition of the cmo^{5}U34 of the tRNA to either C1400 or C1399 with a more or less equal probability. This is the first instance in which a site other than C1400 has been cross-linked, even when different species of tRNA or of ribosomes were used (Ofengand et al., 1986).

Miscoding by the C1401:G1501 Double Mutant. The apparent "wobble" at the decoding site which was detected by the cross-linking studies suggested the possibility that the double mutant might have an increased tendency to misread codons. A way to test this possibility in vitro is to measure the ability of a ribosome to insert leucine into peptide linkage in response to a poly(U) message (Ruusala et al., 1982). This approach has also been used recently by Allen and Noller (1991), who found a modest increase in miscoding due to a C to U mutation at position 1469 in 16S RNA. However, we did not detect any evidence for miscoding when the double mutant was compared to either isolated 30S or a reconstituted synthetic control (Table V). The *E* value, which is a measure of miscoding, was even lower in the double mutant than in the wild-type control. Despite the lack of intrinsic miscoding, the addition of streptomycin, a known inducer of miscoding (Ruusala et al., 1984), was similarly effective in stimulating all three of the samples, causing an approximately 20-fold increase in miscoding by the 30S and wild-type synthetic subunits and at least that much by the double mutant.

DISCUSSION

The Results. This work shows that a specific tertiary base pair in *Escherichia coli* 16S RNA is essential for the proper

Table V: Misincorporation of Leucine Directed by Poly(U) with the C1401:G1501 Double Mutant of 16S RNA

ribosome	streptomycin	Leu × 100[a]	Leu + Phe[a]	E[b]
30S	–	14.7	10.0	1.5
	+	164.	9.9	16.6
G1401:C1501	–	1.0	4.7	0.2
	+	28.9	6.2	4.7
C1401:G1501	–	0.2	5.6	<0.1
	+	34.6	5.9	5.9

[a] Moles of amino acid incorporated per mole of 30S subunit added per 10 min at 37 °C. The misincorporation assay was carried out as described under Experimental Procedures. Values reported are averages of three time points. Blank values (30S omitted) were subtracted. [b] E is the ratio of (Leu × 100)/(Leu + Phe).

function of the ribosome. When the base pair was broken by mutation of either partner, all functions were lost, but when the base pair was restored in the reverse direction, all but one were regained. In view of the proximity of the base pair to C1400, known to be at the ribosomal decoding site, formation of the base pair may be necessary in some way for proper codon recognition. This could explain why our tRNA binding and peptide bond formation assays (which are codon-dependent) were inhibited by the single mutants which could not form the base pair. While the complementary base pair restored most activities, the ability to form the first peptide bond (fMet-Val synthesis) was not restored. The block appears to be subsequent to formation of the 70S initiation complex because reaction with puromycin was not affected. Since the next steps leading to fMet-Val synthesis are binding of Val-tRNA to the A site and peptide bond formation, one or the other of these steps should be defective. However, assays of peptide bond formation (polyphenylalanine synthesis) did not show any inhibition nor did the direct assay of A-site binding. This apparent paradox may be resolved by considering the state of the A site when the first peptide bond is formed versus that during subsequent elongation. As pointed out by Nierhaus and co-workers (Hausner et al., 1988; Nierhaus, 1990), the E site is empty when the A site is initially occupied (A_i in Figure 5) but is filled during subsequent rounds of elongation (A_e). A_i and A_e sites differ in several respects (Nierhaus, 1990). Thus the effect of the reversed base pair could be understood in terms of an ability to properly form an A_i site, while having no effect on an A_e site.

Alternatively, the C1401:G1501 double mutant could be deficient in some aspect of translational fidelity. This may not be detectable in the tRNA binding or polyphenylalanine assays used but could be manifested in an ability to properly match the second codon, GUU, with Val-tRNA. The cross-linking results support the concept of a "sloppy" fit around the anticodon, but the misincorporation assay did not support this view. An increase in frame-shifting is another possibility. Whatever the explanation, the fact that fMet-Val synthesis does not return in the double mutant may explain why so far only the A:U substitution has been found in nature. It will be interesting to determine whether the A1401:U1501 base pair only works in mitochondrial ribosomes or whether that double mutant will be functional in *E. coli* as well.

It has been suggested that the inactivating effect of substitution of G1401 (Cunningham et al., 1992) might be due to a required interaction with U33 of the tRNA anticodon. This U residue is highly conserved in tRNA structures, and its substitution by other nucleotides has been shown to affect rates of reaction with the ribosomes that are involved in codon recognition (Dix et al., 1986). Moreover, the coaxial stacking model of Noller (1986) would place U33 and G1401 in juxtaposition. However, the fact that mutation of C1501 to G can reverse the effect of the G1401 to C mutation suggests that the U33–G1401 interaction probably does not occur.

We previously reported that mutation of G1401 to C, U, or A decreased the ability to associate with the 50S subunit (Cunningham et al., 1992). A similar effect was also noted here for the G1501 mutant. Moreover, in agreement with the restoration of the other functional activities in the double mutant, subunit association activity was also restored (Table III). This is most clearly seen by comparing the expected value of the double mutant, 25%, with the 90% experimentally found. While it was initially surprising that mutations which affect tRNA binding to the 30S subunit also block subunit association, various reports in the literature have already suggested the existence of some sort of subtle connection between tRNA binding and subunit association [cited in Noller (1991) and in Cunningham et al. (1992)]. Moreover, Mitchell et al. (1992) have detected a zero-length UV cross-link between residues 1408–1411 and a site in 23S RNA, indicating a physical closeness of these residues to the 50S subunit. Our results reinforce this set of observations.

The Model. The base pair confirmed by these studies to be functionally important is shown as (b) in Figure 8, left panel. The other tertiary base pairs proposed by Gutell and Woese (1990) are indicated as (c) and as the lower one of the (a) doublet. The upper base pair shown in (a) is universally found as is the one proposed for C1407:G1494 (see Figure 9A). Thus, these latter two cannot be verified by comparative sequence analysis. However, the upper base pair in (a) has been verified as functionally important by similar single and double mutant constructions of the type described in this work (Cunningham et al., 1990a). Base pair (c) is currently under study in our laboratory. Preliminary evidence suggests an interaction here also, although in this case the effect appears as a negative cooperativity (A. Bakin and J. Ofengand, unpublished results). This tertiary base pair is particularly interesting as its nearness to helices 28 and 45 (Figure 8) imposes considerable steric restraints on this region of the ribosome.

As shown in the ribosome model in Figure 8, the two single-stranded RNA sequences are believed to lie approximately on either side of the cleft. Depending on the exact location, it may be necessary to bridge the cleft in some manner, either by invoking movement of the platform relative to the body or by looping out the RNA sequences so as to span the cleft. Note, however, that the detailed structure of the 30S subunit, including the cleft region, is still a matter of debate (Vasiliev et al., 1983; Gornicki et al., 1984; Stöffler-Meilicke & Stöffler, 1990; Frank et al., 1991). Such uncertainties about the details of ribosome structure do not alter the fact that the results reported here provide the first experimental evidence for the existence of a functionally essential interaction, by tertiary base pair formation, between the two conserved single-stranded RNA segments at the decoding site of the ribosome.

The Tertiary Base Pair Interaction. The four tertiary base pair interactions of Figure 8 are shown in more detail in Figure 9 along with the additional universal base pair 1407:1494. Other potential base pairs are indicated by dotted lines. These latter pairs are not always present but *may* form in a few instances as indicated to buttress adjacent tertiary base pairs. All of the tertiary pairs are either universal or true compensating base pairs. It is worthy of note that the relative positions of purines and pyrimidines are never exchanged and that the five tertiary pairs are CG or GC in a strictly alternating pattern. The structure in panel B is an attempt to construct an alternate

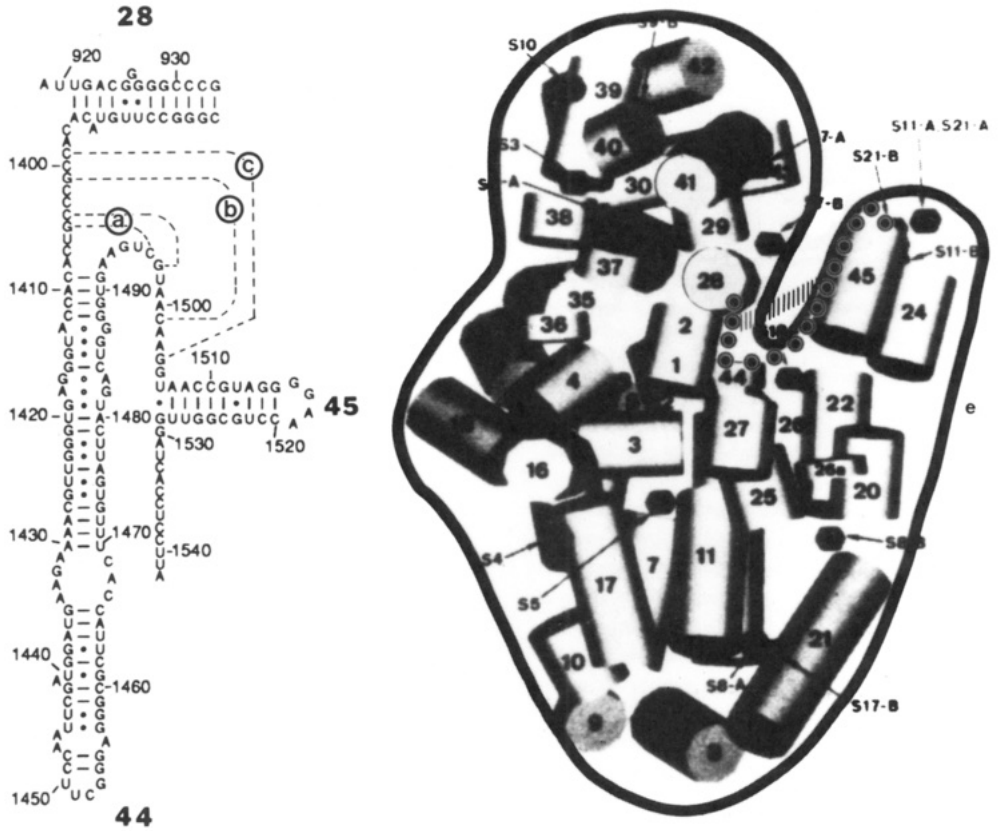

FIGURE 8: Model for the interaction of the conserved sequences around position 1400 with the conserved sequence around position 1500. (Left panel) Sequence of the 3′ minor domain showing helices 28, 44, and 45 which are connected by the two single-stranded sequences. Four base-pair interactions, a, b, and c, are shown. (Right panel) Three-dimensional arrangement of the helices of 16S RNA within the 30S ribosome according to Schüler and Brimacombe (1988). An outline of the 30S subunit (Gornicki et al., 1984; Stöffer-Meilicke & Stöffler, 1990) has been superimposed on the Brimacombe model, and dots have been added to illustrate in a schematic way how the two single-stranded sequences connect the helices. The shaded bar symbolizes the base–base interactions indicated as b and/or c in the left panel.

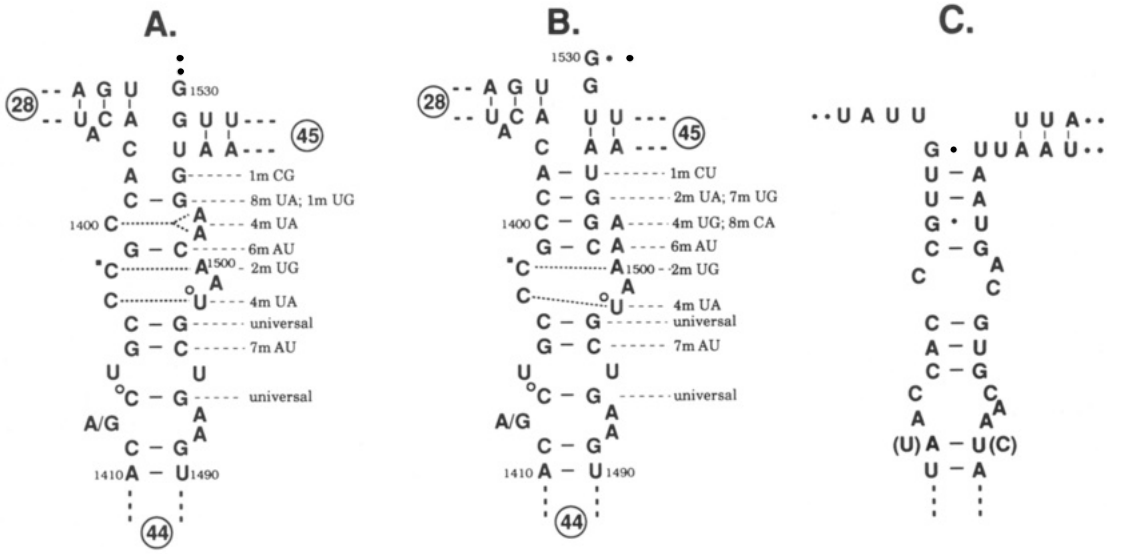

FIGURE 9: Proposed tertiary interactions between the 1397–1408 and 1492–1505 conserved single-stranded sequences of *E. coli* 16S ribosomal RNA. The sequences shown are invariant in the cytoplasmic ribosomes of all eukaryotes, archaebacteria, and eubacteria, in the ribosomes of all but two chloroplasts, and in some mitochondrial ribosomes. The variations indicated on the figure have been found so far only in other species of mitochondrial ribosomes. The number and type of each variation are indicated, with m referring to mitochondrial. The circled numbers refer to the helices of Figure 8. ■C, °C, and °U are m^4Cm, m^5C, and m^3U, respectively. (Panel A) Tertiary interactions shown as solid lines as proposed by Gutell et al. (1985) and Gutell and Woese (1990). The interactions indicated by the dotted lines *could* occur in a few cases, as indicated. (Panel B) As in panel A but pairing C1400 with G1504, C1399 with G1505, and A1398 with U1506. (Panel C) Equivalent sequence region for four species of trypanosome kinetoplasts aligned by manual inspection of the sequences (Neefs et al., 1991).

pairing arrangement. It differs in that C1400 is paired with G1504, creating a bulge on only one side of the helix. This allows pairing of C1399 with G1505 and A1398 with U1506. While this arrangement is suitable for those organisms which have conserved both sequences, it does not fit so well to the mitochondrial data, nor does it explain why C1400 should be so readily cross-linked to tRNA. The structure in panel A, with a looped out C1400, makes this reaction more plausible. In panel C, the equivalent region of the four known small subunit RNA sequences from trypanosome kinetoplasts is

arranged so as to be similar to panels A and B. It is intriguing that, despite the major diversion of sequence, a similar overall picture emerges.

Although the emphasis in this paper has been on the need for tertiary base pair formation to maintain function, it does not necessarily follow that the base pairs per se are the essential element. For example, one could postulate that the base pairs are only important for generating the 1–3 nucleotide loops shown in Figure 9, which are the critical interacting elements.

Is the Tertiary Base Pair Present All the Time? The possibility was already mentioned that tertiary base pair formation may be only a transient phenomenon, albeit necessary for the functioning of the ribosome. An indication that the single-stranded regions around positions 1400 and 1500 are not always juxtaposed has recently been provided by Doring et al. (1992). These authors were able to obtain several zero-length cross-links between the 1393–1403 region and the 1498–1506 sequence in 30S subunits but not in 70S particles. In the latter case, cross-linking from the 1393–1401 sequence was to tRNA which apparently remained bound to the isolated 70S particles. This finding is not inconsistent with our results, which show a need for the tertiary base pair to obtain tRNA binding to the P and A sites of 70S ribosomes. While the base-paired structure might be needed for tRNA to bind, *once bound* the base pairs, or for that matter the entire interaction between the two single strands (Figure 9), could be disrupted. It is even possible to speculate that the periodic disruption and re-formation of the interactions(s) are essential elements in the repetitive act of codon recognition during protein synthesis. The same mechanism may also be operative in 30S initiation complex formation, as suggested by our function studies. This would not have been detected by Döring et al. since their 30S subunits were free of bound tRNA.

Additional evidence for the transient nature of the G1401:C1501 base pair is the recent report that the 1397–1404 region is available for binding with complementary oligodeoxynucleotides (Weller & Hill, 1992) as well as earlier reports that in the ribosome the N_7 of G1401 (Moazed et al., 1986a), the N_3 of C1501 (Moazed et al., 1986b), and the phosphate of G1401 (Baudin et al., 1989) are exposed to structure-probing reagents.

Four RNA Molecules at the Decoding Site. The picture that is beginning to emerge from our studies is that of a rather densely packed region of ribosomal RNA at the decoding site of the ribosome (Figure 10). This schematic two-dimensional view of what is a three-dimensional object is intended to convey a sense of the stereochemical constraints operative in this region rather than to be an accurate representation of the location of each molecule. The figure shows the cleft and large projection of the *E. coli* 30S subunit (Gornicki et al., 1984) in outline form. The approximate location and orientation of helices 28, 44, and 45 of the 3′-end of 16S RNA in the 30S subunit are derived from the three-dimensional models of Brimacombe et al. (1988) and Stern et al. (1988), which in turn are based on a large body of previous data. The placement of the 3′-end and connecting single strand of rRNA to helix 45 is in keeping with the immunoelectron microscopic localization of the 3′-terminus [referenced in Gornicki et al. (1984)]. The 1400- and 1500-region single strands are arranged as in Figure 9A. The arrangement of mRNA, exemplified by ϕRH mRNA, is designed to show a maximal Shine–Dalgarno pairing. Placement of the initiating AUG is constrained by the need to juxtapose the 5′ anticodon base of P-site-bound tRNA to C1400 of the rRNA, in view of the

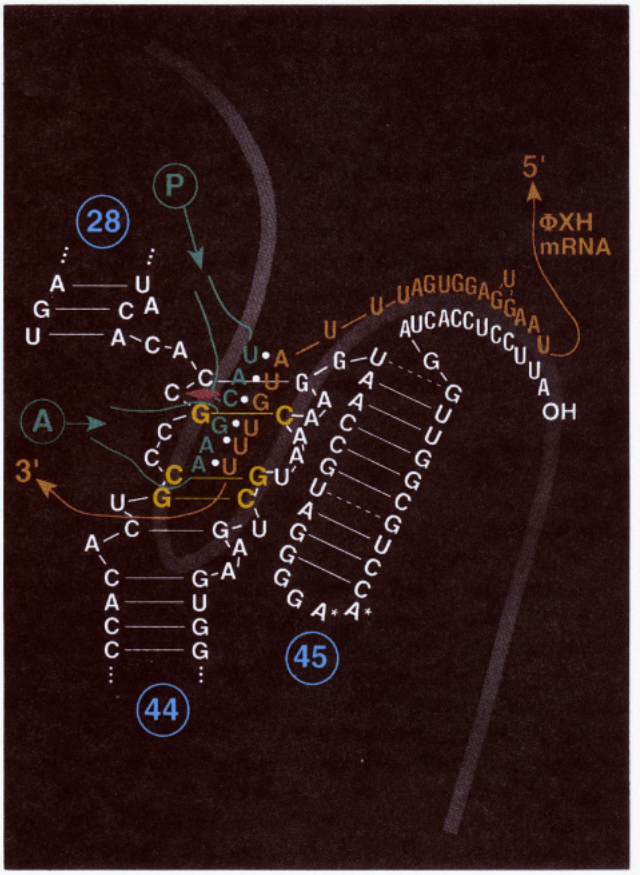

FIGURE 10: Schematic version of the arrangement of tRNAs, mRNA, and rRNA around the decoding site of the ribosome. See text for explanation.

cyclobutane dimer cross-link (diamond) which can be formed there (Ofengand et al., 1986). This allows a distance of only 20 Å (two unapired nucleotides) between the 3′-end of the Shine–Dalgarno sequence and the A of the AUG (Gornicki et al., 1984). The A-site tRNA is placed so that its anticodon is adjacent to that of the P site in the direction required by the 5′ to 3′ direction of mRNA translation. The widths of helices 28, 44, and 45 and the tertiary base pairs between the 1400 and 1500 regions are approximately correctly proportioned to the scale indicated by the outline of the ribosomal surface. The codon–anticodon base pairs are *not* shown in their true size in this two-dimensional representation but are only indicated schematically. The constraint on the distance between the initiatior AUG and the Shine–Dalgarno region implicit in this diagram provides additional evidence for the juxtaposition of the large projection and the head of the 30S subunit at some stage(s) of translation.

ACKNOWLEDGMENT

We thank Robin Gutell, University of Colorado, for sharing his compilation of published and unpublished sequences of 16S RNA and for pointing out the potential for base pairing between positions 1402 and 1500.

REFERENCES

Allen, P. N., & Noller, H. F. (1991) *Cell 66*, 141–148.
Bakin, A., & Ofengand, J. (1992) *BioTechniques* (in press).
Baudin, F., Mougel, M., Romby, P., Eyermann, F., Ebel, J.-P., Ehresmann, B., & Ehresmann, C. (1989) *Biochemistry 28*, 5847–5855.
Brimacombe, R., Atmadja, J., Stiege, W., & Schüler, D. (1988) *J. Mol. Biol. 199*, 115–136.

Cunningham, P. R., Weitzmann, C., Nègre, D., Sinning, J. G., Frick, V., Nurse, K., & Ofengand, J. (1990a) in *The Ribosome. Structure, Function, and Evolution* (Hill, W., Dahlberg, A., Garrett, R., Moore, P., Schlessinger, D., & Warner, J., Eds.) pp 243–252, American Society for Microbiology, Washington, DC.

Cunningham, P. R., Weitzmann, C. J., Nurse, K., Masurel, R., van Knippenburg, P. H., & Ofengand, J. (1990b) *Biochim. Biophys. Acta 1050*, 18–26.

Cunningham, P. R., Pflumm, M., Weitzmann, C. J., Nurse, K., & Ofengand, J. (1991a) *J. Cell. Biochem. 15D*, 177.

Cunningham, P. R., Weitzmann, C. J., Nurse, K., Pflumm, M., & Ofengand, J. (1991b) Abstracts, 15th International Congress of Biochemistry, Jerusalem, Israel, p 110.

Cunningham, P. R., Weitzmann, C. J., & Ofengand, J. (1991c) *Nucleic Acids Res. 19*, 4669–4673.

Cunningham, P. R., Richard, R. B., Weitzmann, C. J., Nurse, K., & Ofengand, J. (1991d) *Biochimie 73*, 789–796.

Cunningham, P. R., Nurse, K., Weitzmann, C. J., Nègre, D., & Ofengand, J. (1992) *Biochemistry 31*, 7629–7637.

Denman, R., Colgan, J., Nurse, K., & Ofengand, J. (1988) *Nucleic Acids Res. 16*, 165–178.

Denman, R., Nègre, D., Cunningham, P. R., Nurse, K., Colgan, J., Weitzmann, C., & Ofengand, J. (1989a) *Biochemistry 28*, 1012–1019.

Denman, R., Weitzmann, C., Cunningham, P. R., Nègre, D., Nurse, K., Colgan, J. Pan, Y.-C., Miedel, M., & Ofengand, J. (1989b) *Biochemistry 28*, 1002–1011.

Dix, D. B., Wittenberg, W. L., Uhlenbeck, O. C., & Thompson, R. C. (1986) *J. Biol. Chem. 261*, 10112–10118.

Döring, T., Greuer, B., & Brimacombe, R. (1992) *Nucleic Acids Res. 20*, 1593–1597.

Ehresmann, C., & Ofengand, J. (1984) *Biochemistry 23*, 438–445.

Ericson, G., & Wollenzien, P. (1988) *Anal. Biochem. 174*, 215–223.

Frank, J., Penczek, P., Grassucci, R., & Srivastava, S. (1991) *J. Cell Biol. 115*, 597–605.

Gornicki, P., Nurse, K., Hellmann, W., Boublik, M., & Ofengand, J. (1984) *J. Biol. Chem. 259*, 10493–10498.

Gutell, R. R., & Woese, C. R. (1990) *Proc. Natl. Acad. Sci. U.S.A. 87*, 663–667.

Gutell, R. R., Weiser, B., Woese, C. R., & Noller, H. J. (1985) in *Nucleic Acid Research and Molecular Biology* (Cohn, W. E., & Moldave, K., Eds.) Vol. 32, pp 155–216, Academic Press, New York.

Hausner, T.-P., Geigenmüller, U., & Nierhaus, K. H. (1988) *J. Biol. Chem. 263*, 13103–13111.

Hershey, J. W. B. (1987) in *Escherichia coli and Salmonella typhimurium. Cellular and molecular biology* (Neidhardt, F. C., Ingraham, J. L., Low, K. B., Magasanik, B., Schaecter, M., & Umbarger, H. E., Eds.) Vol. 1, pp 613–647, American Society for Microbiology, Washington, DC.

Hui, A. S., Eaton, D. H., & de Boer, H. A. (1988) *EMBO J. 7*, 4383–4388.

Kryzosiak, W., Denman, R., Nurse, K., Hellmann, W., Boublik, M., Gehrke, C. W., Agris, P. F., & Ofengand, J. (1987) *Biochemistry 26*, 2353–2364.

Krzyzosiak, W. J., Denman, R., Cunningham, P. R., & Ofengand, J. (1988) *Anal. Biochem. 175*, 373–385.

Mitchell, P., Osswald, M., & Brimacombe, R. (1992) *Biochemistry 31*, 3004–3011.

Moazed, D., & Noller, H. F. (1989) *Nature 342*, 142–148.

Moazed, D., Van Stolk, B. J., Douthwaite, S., & Noller, H. F. (1986a) *J. Mol. Biol. 191*, 483–493.

Moazed, D., Stern, S., & Noller, H. F. (1986b) *J. Mol. Biol. 187*, 399–416.

Neefs, J.-M., Van de Peer, Y., De Rijk, P., Goris, A., & De Wachter, R. (1991) *Nucleic Acids Res. 19*, 1987–2007.

Nierhaus, K. H. (1990) *Biochemistry 29*, 4997–5008.

Noller, H. F. (1991) *Annu. Rev. Biochem. 60*, 191–227.

Noller, H. F., Asire, M., Barta, A., Douthwaite, S., Goldstein, T., Gutell, R. R., Moazed, D., Normanly, J., Prince, J. B., Stern, S., Triman, K., Turner, S., Van Stolk, B., Wheaton, V., Weiser, B., & Woese, C. R. (1986) in *Structure, Function, and Genetics of Ribosomes* (Hardesty, B., & Kramer, G., Eds.) pp 143–163, Springer-Verlag, New York.

Noller, H. F., Hoffarth, V., & Zimniak, L. (1992) *Science 256*, 1416–1419.

Nurse, K., Colgan, J., Denman, R., Wilhelm, J., & Ofengand, J. (1987) *Biochimie 69*, 1105–1112.

Ofengand, J., & Liou, R. (1981) *Biochemistry 20*, 552–559.

Ofengand, J., Liou, R., Kohut, J., III, Schwartz, I., & Zimmermann, A. (1979) *Biochemistry 18*, 4322–4332.

Ofengand, J., Gornicki, P., Chakraburtty, K., & Nurse, K. (1982) *Proc. Natl. Acad. Sci. U.S.A. 79*, 2817–2821.

Ofengand, J., Ciesiolka, J., & Nurse, K. (1986) in *Structure and Dynamics of RNA* (van Knippenberg, P. H., & Hilbers, C. W., Eds.) pp 273–287, Plenum Publishing Corp., New York.

Rinke-Appel, J., Jünke, N., Stade, K., & Brimacombe, R. (1991) *EMBO J. 10*, 2195–2202.

Rottmann, N., Kleuvers, B., Atmadja, J., & Wagner, R. (1988) *Eur. J. Biochem. 177*, 81–90.

Ruusala, T., Ehrenberg, M., & Kurland, C. G. (1982) *EMBO J. 1*, 741–745.

Ruusala, T., Andersson, D., Ehrenberg, M., & Kurland, C. G. (1984) *EMBO J. 3*, 2575–2580.

Schüler, D., & Brimacombe, R. (1988) *EMBO J. 7*, 1509–1513.

Schwartz, I., & Ofengand, J. (1978) *Biochemistry 17*, 2524–2530.

Stern, S., Weiser, B., & Noller, H. F. (1988) *J. Mol. Biol. 204*, 447–481.

Stern, S., Powers, T., Changchien, L.-M., & Noller, H. F. (1989) *Science 44*, 783–790.

Stöffler-Meilicke, M., & Stöffler, G. (1990) in *The Ribosome. Structure, Function, and Evolution* (Hill, W., Dahlberg, R., Garett, P., Moore, D., Schlessinger, D., & Warner, J., Eds.) pp 123–133, American Society for Microbiology, Washington, DC.

Tate, W., Greuer, B., & Brimacombe, R. (1990) *Nucleic Acids Res. 18*, 6537–6544.

Thomas, G., Gregory, R. J., Winslow, G., Muto, A., & Zimmerman, R. A. (1988) *Nucleic Acids Res. 16*, 8129–8146.

Vasiliev, V. D., Selivanova, O. M., Baranov, V. I., & Spirin, A. S. (1983) *FEBS Lett. 155*, 167–172.

Weller, J. W., & Hill, W. E. (1992) *Biochemistry 31*, 2748–2757.

Zamir, A., Miskin, R., Vogel, Z., & Elson, D. (1974) *Methods Enzymol. 30*, 406–426.

Registry No. Cytosine, 71-30-7; guanine, 73-40-5; adenine, 73-24-5; uracil, 66-22-8.